Application of Steady-State Integral Proportional Integral Controller for Inner Dynamics Control Loop of Multi-rotor UAVs

Jun Jet Tai
School of Engineering
Taylor's University
Selangor, Malaysia
junjet.tai02@taylors.edu.my

Swee King Phang
School of Engineering
Taylor's University
Selangor, Malaysia
sweeking.phang@taylors.edu.my

Choon Lih Hoo
School of Engineering
& Physical Sciences
Heriot-Watt University Malaysia
Putrajaya, Malaysia
c.hoo@hw.ac.uk

***Abstract*—The industry usage for racing grade multi-rotors have not yet been widely probed. These multi-rotors focus on maximizing system actuation whilst minimizing system overshoot and oscillations. These systems usually employ cascaded PID control loops, and are generally largely tuned by hand. This paper presents a novel control method adapted from steady state integral methods derived from direct current motors in order to develop a new control scheme for racing grade multi-rotors. The performance of this controller was tested on a quad-rotor non-linear dynamic model simulator. The controller shows good robustness and performance which is evidenced from the very small magnitude error under the influence of disturbance, while making tuning intuitive and simple.**

***Index Terms*—UAV, Steady-State Integral, PI Control**

I. Introduction

The multi-rotor system is a system of parallel facing rotors with fixed pitch in an orientation about a similar plane. The fixed pitch of a multi-rotor propulsion system makes it mechanically simpler than an ordinary helicopter. Due to the orientation of the rotors, these systems are able to be very agile in movement, but are inherently unstable. These characteristics make the multi-rotor system capable of performing quick and precise maneuvers [1], as well as function as a robotics platform in structured and unstructured environments [2], and also cooperate in payload manipulation [3].

Racing style multi-rotors with realistic industrial applications are not well discovered. The significant translational velocities achievable by these Unmanned Aerial Vehicles (UAVs) can be considered to be advantageous in applications such as rescue, civil defence, surveillance, as well as emergency. Consequently, racing quad rotors are gaining traction in the freestyle flying category, where quad rotors are constructed by the end user utilizing off-the-shelf components from a variety of manufacturers.

Several classical, modern, and artificial intelligence control schemes have been developed for the inner control loop of multi-rotor systems. These control methods include H_∞ PID [4], linear quadratic regulator and linear quadratic Gaussian control [5], and neural network control [6], which has shown good robustness and performance in the control of attitude of the multi-rotor.

The classical cascaded proportional-proportional integral derivative (PPID) controller, however, has been widely used in the racing multi-rotor industry due to the simplicity and ease of implementation for not requiring an accurate mathematical model of the actual system [7]. These controllers are implemented on the onboard computer on racing multi-rotors, and the stock tuning parameters are usually enough to get the multi-rotor in the air [8], but usually require manual tuning by the end user in order to get the performance that is desired.

Many cases of tuning a PID controller involves iterative hand tuning to optimize settling time, steady state error, and overshoot. Some examples include the Ziegler-Nichols step response method [9] and IMC-PID [10] tuning methods. Alternative methods of tuning a PID controller include analytic methods where the system dynamics are known. Such technicalities are usually avoided by the average consumer, and trial and error along with human observations are utilized to determine the right tuning parameters for a given racing multi-rotor. Often, tuning is a matter of balancing controller overshoot with under actuation of the system.

In speed control of direct current motors, there exists a steady state integral analytic method [11], that builds upon the PID control concept to produce a controller where tuning is abated. By studying the physical model of the system, a general controller is designed for direct current motors that minimizes overshoot while allowing refined control of settling time.

Extensive research has been done to simplify the multi-rotor system dynamic equations, the primary methods include utilizing Newton-Euler equations [12] [13] [14], and Euler-Lagrangian methods [15]. In this paper, a steady state integral method of designing a general controller for multi-rotor systems is proposed with the Newton-Euler mathematical model. Through mathematical proof, the steady state controller method allows for the developing of proportional and integral

978-1-5386-7167-2/18/$31.00

gains together by taking into consideration a single system constant. The proposed solution foregoes the derivative portion of PID control, and is therefore more lightweight than a standard PID controller, while offering good robustness and performance.

II. Dynamic Model of Multi-rotor UAV

Fig. 1 depicts the mathematical block diagram representation of a multi-rotor (specifically, quad-rotor) that the control algorithm will be based upon. The dynamic model is split into two parts, an outer loop controller that governs outer loop dynamics, and an inner loop controller that governs inner loop dynamics. Typically, the inner loop controller acts with a smaller loop time than the outer loop controller. The inner loop controller governs the dynamics of position in three rotational degrees of freedom. Whereas the outer loop controller governs the dynamics of the three linear degrees of freedom.

The model overview of the multi-rotor (quad-rotor in this case) UAV is shown in Fig. 2. In the block diagram, the inputs to the UAV, δ_n, are shown on the left. They are the normalized pulse-width modulation (PWM) control signals sent from the flight control board to the motor speed controllers. The linear velocity $\mathbf{V_b} = [u, v, w]^{\mathrm{T}}$, linear position $\mathbf{P_g} = [x, y, z]^{\mathrm{T}}$, Eular angle $\Theta = [\phi, \theta, \psi]^{\mathrm{T}}$, and angular velocity $\omega = [p, q, r]^{\mathrm{T}}$ shown on the right of the block diagram are the output of the system, which will be used on feedback control later (linear position/velocity for position control, angular position/velocity for attitude control). Note that in our mathematical derivation, the quad-rotor UAV has the cross configuration, with rotor number 1, 2, 3, 4 and basic working principle indicated in [12].

A. Kinematic and Rigid-body-dynamics

The translation and rotation motions between the ground frame and the body frame can be related with two well-known navigation equations in Equation (1) and (2). They will be shown here for completeness and will not be further discussed. Detail derivation of these equations are well documented in [16].

$$\dot{\mathbf{P}}_{\mathbf{g}} = \mathbf{R}_{\mathbf{g/b}}\mathbf{V_b}, \tag{1}$$

$$\dot{\Theta} = \mathbf{S}^{-1}\omega, \tag{2}$$

where the rotational matrix, $\mathbf{R_{n/b}}$, and the lumped transformation matrix, $\mathbf{S}^{-1}$ are given by

$$\mathbf{R_{g/b}} = \begin{bmatrix} c_\theta c_\psi & s_\phi s_\theta c_\psi - c_\phi s_\psi & c_\phi s_\theta c_\psi + s_\phi s_\psi \\ c_\theta s_\psi & s_\phi s_\theta s_\psi + c_\phi c_\psi & c_\phi s_\theta s_\psi - s_\phi c_\psi \\ -s_\theta & s_\phi c_\theta & c_\phi c_\theta \end{bmatrix}, \tag{3}$$

$$\mathbf{S}^{-1} = \begin{bmatrix} 1 & s_\phi t_\theta & c_\phi t_\theta \\ 0 & c_\phi & -s_\phi \\ 0 & s_\phi/c_\theta & c_\phi/c_\theta \end{bmatrix}, \tag{4}$$

with $s_* = \sin(*)$, $c_* = \cos(*)$, and $t_* = \tan(*)$. It is worth to note that $\mathbf{R_{b/g}} = \mathbf{R_{g/b}^{-1}} = \mathbf{R_{g/b}^{\mathrm{T}}}$

To describe the translation and rotation dynamics of any rigid-body, Newton-Euler formalism can be expressed as

$$m\dot{\mathbf{V}}_{\mathbf{b}} + \omega \times (m\mathbf{V_b}) = \mathbf{F}, \tag{5}$$

$$\mathbf{J}\dot{\omega} + \omega \times (\mathbf{J}\omega) = \mathbf{M}, \tag{6}$$

where $\mathbf{F}$ and $\mathbf{M}$ are respectively the force and moment vectors acting on the quad-rotor UAV. As the designed quad-rotor UAV is four way symmetrical, the inertia matrix, $\mathbf{J}$, can be assumed diagonal, i.e.,

$$\mathbf{J} = \begin{bmatrix} J_x & 0 & 0 \\ 0 & J_y & 0 \\ 0 & 0 & J_z \end{bmatrix}. \tag{7}$$

B. Forces and Moments

The quad-rotor UAV movements are contributed mostly by the forces and moments generated by the UAV. However, external forces and moments acting on the UAV fuselage do affect its motion in some way. Generally, there are three main sources of forces and moments as mentioned in [12], [17], i.e., the gravitational force, the rotor thrust, and the fuselage drag force due to air speed. In the derivation later, as there is no way to measure speed of wind on-board the UAV, the air speed is assumed to be the ground speed of the UAV, to be given by GPS measurement in actual applications.

As the gravitational force acts directly downwards towards the Earth center, it is assumed to be acting along z-axis of the ground frame. By transforming it to the body frame, we have

$$\mathbf{F_{gravity}} = \mathbf{R_{b/g}} \begin{bmatrix} 0 \\ 0 \\ mg \end{bmatrix} = \begin{bmatrix} -mgs_\theta \\ mgc_\theta s_\phi \\ mgc_\theta c_\phi \end{bmatrix}. \tag{8}$$

Forces and moments generated by the multi-rotor UAV come from its rotors. We can safely assume that there is no flapping dynamics from the rotor, as the rotor diameter is small and the rotor hinge is rigid. In this scenario, each rotating rotor creates a thrust, T_n, and a moment, Q_n, for $n = 1, 2, 3, 4$ along its axis. From the aerodynamics consideration, the thrust and torques produced can be modeled as

$$T_n = \frac{1}{4\pi^2} C_T \rho (2r)^4 \Omega_n^2, \tag{9}$$

$$Q_n = \frac{1}{4\pi^2} C_Q \rho (2r)^5 \Omega_n^2, \tag{10}$$

where C_T and C_Q are the aerodynamic coefficients of the propeller, ρ is the density of the air, r is the radius of the rotor blade. A smart way to simplify the equations would be assuming that the aerodynamic coefficients to be constant, which is generally the case when the collective pitch angle of the blade is fixed. In this way, Equation (9) and (10) can be expressed as

$$T_n = k_T \Omega_n^2, \tag{11}$$

$$Q_n = k_Q \Omega_n^2, \tag{12}$$

where the constants k_T and k_Q to be obtained through experiments.

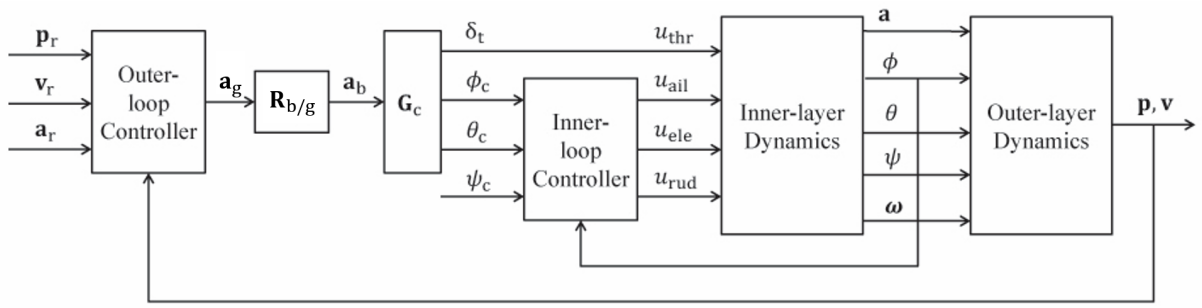

Fig. 1. Overview control structure of the quad-rotor UAV

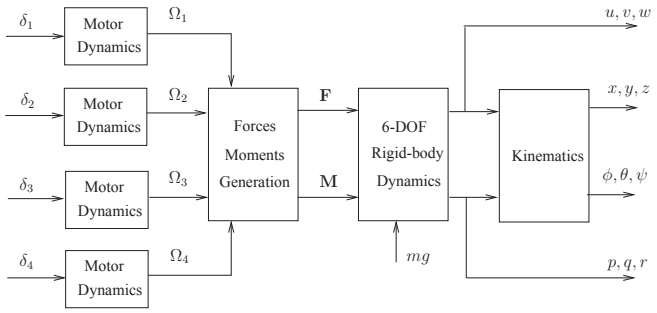

Fig. 2. Overview block diagram of the quad-rotor UAV model

The total thrusts and moments of the quad-rotor UAV due to the interactions between all four motors can then be formulated as follows:

$$\mathbf{F_{rotor}} = \begin{bmatrix} 0 \\ 0 \\ -(T_{m1}+T_{m2}+T_{m3}+T_{m4}) \end{bmatrix}, \quad (13)$$

$$\mathbf{M_{rotor}} = \begin{bmatrix} \frac{\sqrt{2}}{2}l(T_{m2}+T_{m3}-T_{m1}-T_{m4}) \\ \frac{\sqrt{2}}{2}l(T_{m1}+T_{m2}-T_{m3}-T_{m4}) \\ Q_1+Q_3-Q_2-Q_4 \end{bmatrix}. \quad (14)$$

In this work, good performance of the UAV travels at high velocity (10 to 20 m/s) needs to be guaranteed to achieve a speed performance similar to racing drones. Thus in the mathematics model of the UAV, drag force due to air speed needs to be identified. We formulate the drag force as

$$\mathbf{F_{drag}} = \begin{bmatrix} -b_w & 0 & 0 \\ 0 & -b_w & 0 \\ 0 & 0 & 0 \end{bmatrix} \mathbf{V_b}, \quad (15)$$

where b_w is the drag coefficient that will be identified via bench experiment in wind tunnel.

C. Motor Dynamics

A standard electric motor is a 2nd-order system with the consideration of its electrical and mechanical dynamics. The electrical dynamic is, however, much faster than the mechanical dynamic, and thus it is usually sufficient to model motor dynamics to a 1st-order system as shown in [18].

The dynamics of the motor can be formulated as

$$\dot{\Omega}_n = \frac{1}{\tau_m}[k_m(\delta_n - \delta_n^*) - \Omega_n], \quad (16)$$

where the steady state gain, k_m, and time constant, τ_m can be obtained experimentally. Here, δ_n^* is the normalized input trim where the motor starts spinning. Note that in Equation 16, δ_n is the normalized input to the motor speed controller, with the following normalization process,

$$\delta_n = \frac{u_n - 1000}{1000}, \quad (17)$$

where u_n corresponds to the PWM signal fed to the motor speed controller in unit μs. In general, the minimum and maximum possible pulse widths to the electronics are at 1000 μs and 2000 μs respectively.

Typically, the dynamic loops of the quad-rotor is separated to inner- and outer-loop, where inner-loop controls the orientation (angular and angular rate) of the UAV, while the outer-loop controls the location (position and velocity) of the UAV. By combining Equation (6), (7), and (14), we can obtain a nonlinear relationship between the angular accelerations of 3 axes and the inputs to the system, as

$$J_x\dot{p} = u_1 + (J_y - J_z)rq, \quad (18)$$
$$J_y\dot{q} = u_2 + (J_z - J_x)pr, \quad (19)$$
$$J_z\dot{r} = u_3 + (J_x - J_y)pq, \quad (20)$$

where $[u_1, u_2, u_3] = \mathrm{u}$ is the normalized moment input to the system. Here, the angular rate dynamics of the quad-rotor can be easily linearized by applying linearization at equilibrium points of $\omega = [p, q, r]^{\mathrm{T}} = \mathbf{0}$, or simply by a feedback linearization at

$$u_1 = \bar{u}_1 - (J_y - J_z)rq, \quad (21)$$
$$u_2 = \bar{u}_2 - (J_z - J_x)pr, \quad (22)$$
$$u_3 = \bar{u}_3 - (J_x - J_y)pq. \quad (23)$$

Feedback linearization applied here is perfectly fine as long as the quad-rotor system gives a low-noise estimation of angular rates of the UAV, which is usually the case with the help of an extended Kalman filter (EKF). Therefore, within the linear limits of quad-rotor control, the equation of concern

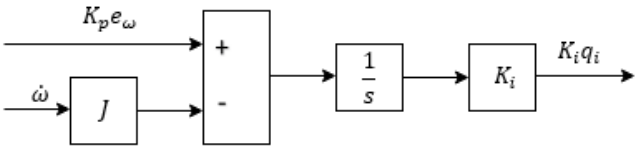

Fig. 3. Proposed PI integral component

for the proposed controller under the influence of a constant external disturbance, $\mathbf{T}$ is given by

$$\mathbf{J}\dot{\omega} \quad = \quad \mathbf{T} + \mathrm{u}. \tag{24}$$

III. Controller Design

Note that the linearized inner-loop system shown in Equation (24) is for all 3 axes. As each of these axis are completely decoupled as a results of linearization (or feedback linearization), we can safely design individual controllers on each direction (yaw, pitch, roll), by considering the multi-rotor rate controller of

$$u \quad = \quad K_p e_w + K_i q_i, \tag{25}$$

on each axis. Here, e_ω is the error of angular velocity, and q_i is the integral of e_ω. Ideally, at steady state, we require the multi-rotor to be at the desired set point with zero steady state error, $\dot{\omega} \to 0$, $e_\omega \to 0$. It is also desirable for q_i to completely compensate for the lack of proportional action, under the influence of K_i. Hence, the controller output from Equation (25) at steady-state would be exactly

$$u = K_i q_{ss} = -T, \tag{26}$$

where q_{ss} is the steady-state integral component. Referencing Equation (24) allows the attainment of

$$K_i q_{ss} \quad = \quad u - J\dot{\omega}, \tag{27}$$

which describes the steady-state input based on signals readily available to a multi-rotor system.

The integral state component referenced in [11] provides an implementable function criterion such that a systems final error value will be zero. This equation is suitably documented. The equation in the Laplace plane is

$$\frac{q_{ss}}{s} - Q(s) \quad = \quad As^n f(s) + B, \tag{28}$$

where A and B are arbitrary constants, and $f(s)$ can be any function based on the signals readily available to a system. Assuming the function used in [11], which is

$$K_i(q_{ss} - q_i) \quad = \quad sq_i, \tag{29}$$

and applying Equation (25) and (27) in the Laplace domain assuming zero initial values, we are able to obtain

$$q_i \quad = \quad (1/s)(K_p e_\omega - J\omega s) \tag{30}$$

The proposed integral component of the rate PI controller therefore becomes the block set indicated in Fig. (3).

The controller can be further simplified by taking the time domain equation for controller output and solving for the integral.

$$\begin{aligned} u &= K_p e_\omega + K_i \int (K_p e_\omega - J\dot{\omega})\, dt \\ &= K_p e_\omega + K_i K_p \int e_\omega \, dt - K_i J\omega. \end{aligned} \tag{31}$$

The resulting dynamics controller from Equation (31) becomes Fig. 4 which can be simplified equivalently into Fig. 5. The corresponding error dynamics equation of the closed-loop controller becomes

$$\theta = \frac{s\frac{1}{J}T + \frac{1}{J}K_p(s + K_i)\theta_r}{s^3 + s^2(\frac{J_m}{J}K_i + \frac{1}{J}K_p) + s(\frac{1}{J}K_pK_i + \frac{1}{J}K_p) + \frac{1}{J}K_pK_i}. \tag{32}$$

Ideally, $J_m = J$ if system identification can be done perfectly. θ_r is the angular reference to the multi-rotor system. In Fig. 5, $K_1 = K_p \cdot K_i$ and $K_2 = K_i \cdot J_m$.

IV. Stability Analysis

To study the stability of the system, the poles of the transfer function are looked at. In this section, two different scenario of the system will be investigated, i.e., in ideal case $J_m = J$, and in non-ideal case $J_m \approx J$ but not exactly J.

A. Ideal Case, $J_m = J$

Assuming $J_m = J$, the closed-loop characteristic of the systems can be perfectly factorized to

$$c(s) \quad = \quad (s + K_i)(s^2 + (K_p/J)s + K_p/J). \tag{33}$$

One can observe that the system is stable as long as $K_i > 0$ and $K_p/J > 0$. In general, the moment of inertia, J, is in the scale of 10^{-3} to 10^{-6} kgm^2 for small scale UAVs. As a result, the third pole, $s = -K_i$, will be much more negative than the other two poles, which approximates the system to be a second order system dominated by $s^2 + (K_p/J)s + K_p/J$. In particular, the system will start to oscillate when $K_p < 4J$.

B. Non-Ideal Case, $J_m \approx J$

Taking the scenario where $J_m \approx J$, perfectly factorizing the characteristic equation is not possible. Two factors are considered when considering the stability of the system from a pole plot point of view, i.e., imaginary component, positive or negative s-plane placement. The Routh table can be utilized in this case to study the latter factor. We begin by forming the Routh table:

Routh Table of Equation (32)

	Column 1	**Column 2**
s^3	1	$\frac{1}{J}K_pK_i + \frac{1}{J}K_p$
s^2	$\frac{J_m}{J}K_i + \frac{1}{J}K_p$	$\frac{1}{J}K_pK_i$
s^1	A	0
s^0	$\frac{1}{J}K_pK_i$	0

where

$$A = (\frac{J_m}{J}K_i + \frac{1}{J}K_p)(\frac{1}{J}K_pK_i + \frac{1}{J}K_p) - \frac{1}{J}K_pK_i. \tag{34}$$

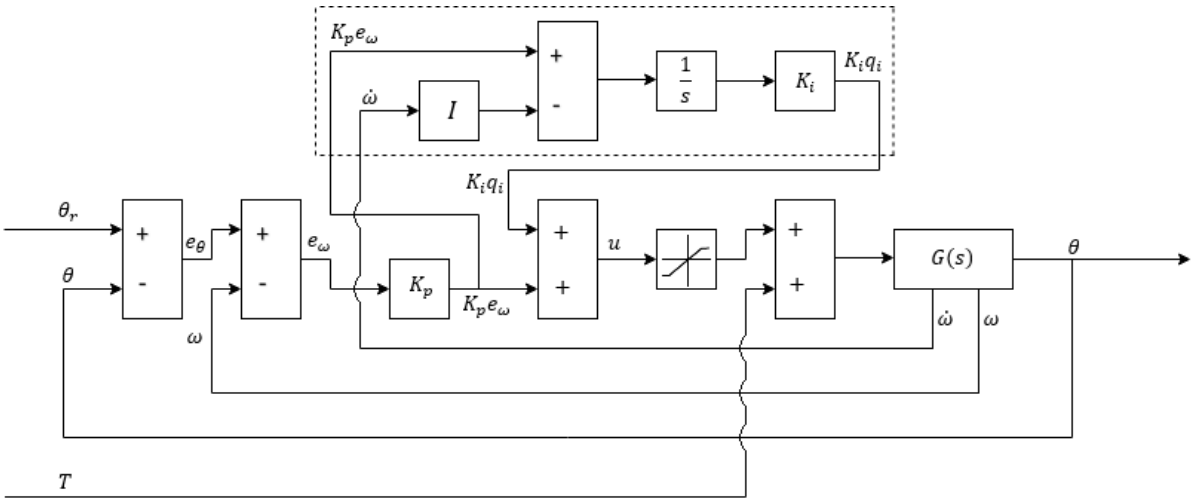

Fig. 4. Angular dynamics control block diagram

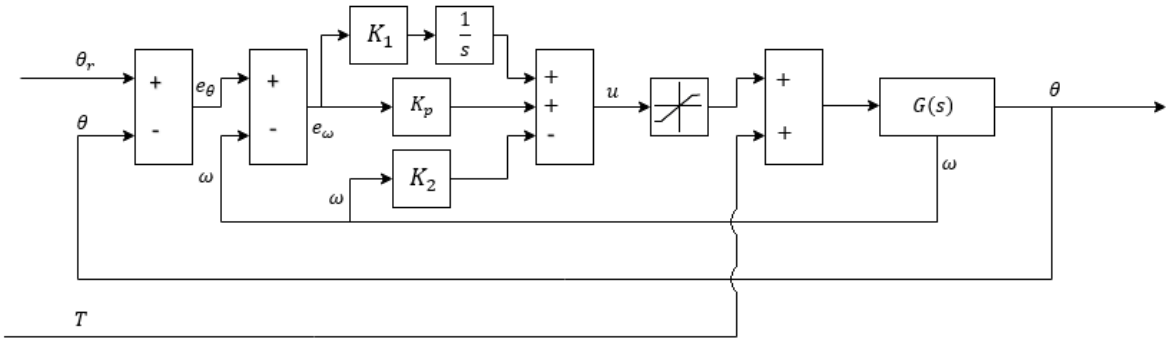

Fig. 5. Finalized angular dynamics control block diagram

With the exception of A, all of the constants on Column 1 are positive. Hence, for all the poles of the system to reside in the left half of the s-plane, it is required that $A > 0$. This criteria can be simplified into

$$J_m > J\frac{1}{K_i + 1} - \frac{K_p}{K_i}. \tag{35}$$

A simplified criterion equation that can be considered is

$$\frac{J_m}{J} > \frac{1}{K_i + 1}, \tag{36}$$

which is not a strict condition, but is sufficient enough to provide stability for the system. In practice, the system will always be stable when $J_m > J$. In scenarios where $J_m < J$, system instability can be overcome by increasing the integral gain.

V. Results

A non-linear simulated model of the quad-rotor UAV is developed in MATLAB environment, based on the mathematical model identified in Section II. The proposed controller is designed based on linearized model, and it is then implemented to the simulator to test its performance. Note that in this simulator, the parameters of the UAV are extracted from T-Lion from the National University of Singapore [19].

Both cases with $J_m = J$ and $J_m \neq J$ are tested, together with an input disturbance T generated as gust input. Fig. 6 and 7 show the step response on the angle of the UAV in both cases. In the second case, J_m is set to be half of J to test the robustness of the controller. In both cases, it is shown that the controller does successfully eliminate any constant angular acceleration disturbance, with minor chattering occurs in both cases. In the case where the parameter J is not accurately identified, the amount of chatter is increased but the controller is still able to suppress it to remain almost 0 angular error. The comparison between the angular error of these cases can seen in Fig. 8. In the case of non-ideal J, although the angular error over time performance is not as good as the ideal case, but the largest error is bounded within 0.05 rad in the presence of constant wind acceleration disturbance.

VI. Conclusion

A novel PI based controller derived from steady state integral methods have been proposed for the multi-rotor dynamical system. Tuning methodology for the controller has been

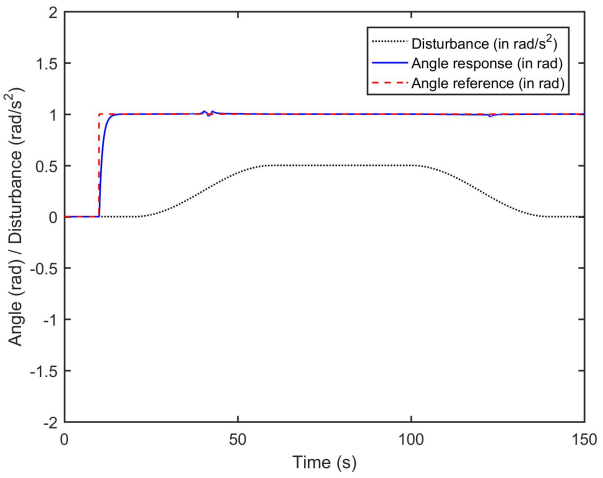

Fig. 6. Step response of the system when $J_m = J$

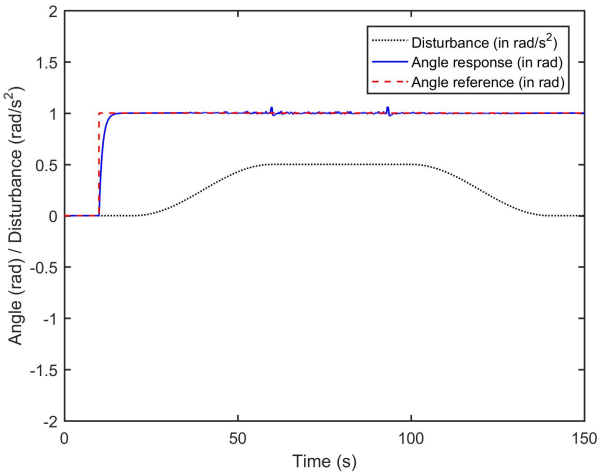

Fig. 7. Step response of the system when $J_m = 50\%J$

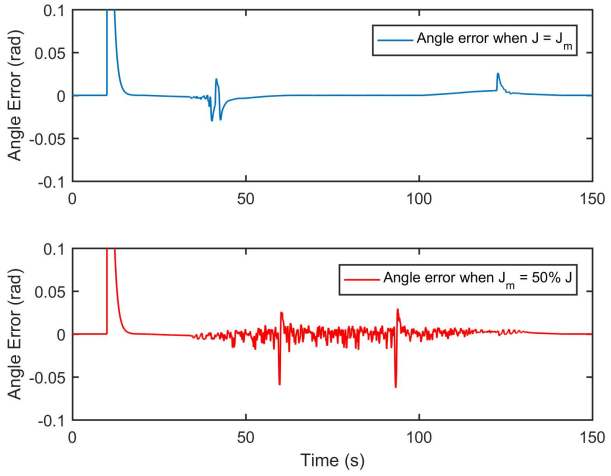

Fig. 8. Comparison of angle error for both cases

derived from mathematical methods, and the methodology is deemed intuitive. The controller was tested on a multi-rotor simulator that represents a highly accurate non-linear model for quad-rotors. The simulation was utilized to study the behaviour of the controller for setpoint tracking under an external influence, and uncertainty within the controller. The controller shows good robustness and performance under the influence of an external disturbance, as well as being able to follow the setpoint closely.

REFERENCES

[1] D. Mellinger, N. Michael, and V. Kumar, "Trajectory generation and control for precise aggressive maneuvers with quadrotors," *The International Journal of Robotics Research*, vol. 31, no. 5, pp. 664–674, 2012.

[2] M. Achtelik, A. Bachrach, R. He, S. Prentice, and N. Roy, "Stereo vision and laser odometry for autonomous helicopters in gps-denied indoor environments," in *SPIE Unmanned Systems Technology XI*, vol. 7332, 2009.

[3] M. Bloandsch, S. Weiss, D. Scaramuzza, and R. Siegwart, "Vision based mav navigation in unknown and unstructured environments," in *International Conference on Robotics and Automation 2010*, pp. 21–28, IEEE, 2010.

[4] J. P. Ortiz, L. I. Minchala, and M. J. Reinoso, "Nonlinear robust h-infinity pid controller for the multivariable system quadrotor," *IEEE Latin America Transactions*, vol. 14, no. 3, pp. 1176–1183, 2016.

[5] H. Purnawan, E. B. Purwanto, *et al.*, "Design of linear quadratic regulator (lqr) control system for flight stability of lsu-05," in *Journal of Physics: Conference Series*, vol. 890, p. 012056, IOP Publishing, 2017.

[6] P. Burman *et al.*, *Quadcopter stabilization with neural network*. PhD thesis, University of Texas at Austin, 2016.

[7] J. Ren, D.-X. Liu, K. Li, J. Liu, Y. Feng, and X. Lin, "Cascade pid controller for quadrotor," in *Information and Automation (ICIA), 2016 IEEE International Conference on*, pp. 120–124, IEEE, 2016.

[8] D. Brescianini, M. Hehn, and R. DAndrea, "Nonlinear quadrocopter attitude control," in *ETH Zurich Research Collection*, ETH Zurich, 2013.

[9] K. J. Åström and T. Hägglund, "Revisiting the ziegler–nichols step response method for pid control," *Journal of process control*, vol. 14, no. 6, pp. 635–650, 2004.

[10] A. T. Azar and F. E. Serrano, "Robust imc–pid tuning for cascade control systems with gain and phase margin specifications," *Neural Computing and Applications*, vol. 25, no. 5, pp. 983–995, 2014.

[11] C. L. Hoo, S. M. Haris, E. C. Y. Chung, and N. A. N. Mohamed, "Steady-state integral proportional integral controller for pi motor speed controllers," *Journal of Power Electronics*, vol. 15, no. 1, pp. 177–189, 2015.

[12] S. K. Phang, K. Li, K. H. Yu, B. M. Chen, and T. H. Lee, "Systematic design and implementation of a micro unmanned quadrotor system," *Unmanned Systems*, vol. 2, no. 02, pp. 121–141, 2014.

[13] A. Nemati and M. Kumar, "Modeling and control of a single axis tilting quadcopter," in *2014 American Control Conference*, IEEE, 2014.

[14] Z. Benic, P. Piljek, and D. Kotarski, "Mathematical modelling of unmanned aerial vehicles with four rotors," in *Interdisciplinary Description of Complex Systems*, vol. 14, pp. 88–100, INDEC, 2016.

[15] T. Luukkonen, "Modelling and control of quadcopter," *Independent research project in applied mathematics, Espoo*, vol. 22, 2011.

[16] G. Cai, B. M. Chen, and T. H. Lee, *Unmanned rotorcraft systems*. Springer Science & Business Media, 2011.

[17] S. K. Phang, K. Li, F. Wang, B. M. Chen, and T. H. Lee, "Explicit model identification and control of a micro aerial vehicle," in *Unmanned Aircraft Systems (ICUAS), 2014 International Conference on*, pp. 1048–1054, IEEE, 2014.

[18] K. Li, S. K. Phang, B. M. Chen, and T. H. Lee, "Platform design and mathematical modeling of an ultralight quadrotor micro aerial vehicle," *Communications*, vol. 1, no. 2, p. 23, 2013.

[19] K. Peng, F. Lin, S. K. Phang, and B. M. Chen, "Nonlinear flight control design for maneuvering flight of quadrotors in high speed and large acceleration," in *Unmanned Aircraft Systems (ICUAS), 2018 International Conference on*, pp. 212–221, IEEE, 2018.